Neutron contribution to nuclear deeply virtual Compton scattering asymmetries

V. Guzey*
Theory Center, Jefferson Laboratory, Newport News, Virginia 23606, USA
(Received 7 March 2008; published 19 August 2008)

Using a simple model for nuclear generalized parton distributions (GPDs), we study the role of the neutron contribution to nuclear deeply virtual Compton scattering (DVCS) observables. As an example, we use the beam-spin asymmetry $A_{\rm LU}^A$ measured in coherent and incoherent DVCS on a wide range of nuclear targets in the HERMES and JLab kinematics. We find that at small values of the momentum transfer t, $A_{\rm LU}^A$ is dominated by the coherent-enriched contribution, which enhances $A_{\rm LU}^A$ compared to the free proton asymmetry $A_{\rm LU}^p$, $A_{\rm LU}^A(\phi)/A_{\rm LU}^p(\phi) = 1.8$–$2.2$. At large values of t, the nuclear asymmetry is dominated by the incoherent contribution and $A_{\rm LU}^A/(\phi)A_{\rm LU}^p(\phi) = 0.66-0.74$. The deviation of $A_{\rm LU}^A(\phi)/A_{\rm LU}^p(\phi)$ from unity at large t is a result of the neutron contribution, which gives a possibility to constrain neutron GPDs in incoherent nuclear DVCS. A similar trend is expected for other DVCS asymmetries.

DOI: 10.1103/PhysRevC.78.025211 PACS number(s): 13.60.−r, 24.85.+p, 25.30.Rw

I. INTRODUCTION

Hard exclusive reactions such as deeply virtual Compton scattering (DVCS), $\gamma^* T \to \gamma T'$, and hard exclusive meson production (HEMP), $\gamma^* T \to M T'$, have emerged as indispensable tools to access the microscopic (parton) properties of hadrons [1–14]. In the above reactions, T and T' stand for any hadronic target (nucleon, pion, atomic nucleus); M denotes any meson. Note that the above reactions may also include transitions between different hadronic states such as, e.g., $N \to \Delta$, $p \to n$, $N \to N\pi$ [15–17] and production of pairs of mesons [18,19].

In addition, "inverse" hard exclusive reactions such as $\gamma N \to \gamma^* N \to l^+ l^- N$ [20] and $\pi N \to \gamma^* N \to l^+ l^- N$ [21], and "u-channel" reactions such as $\gamma^* \gamma \to \pi\pi$ [22] were investigated.

In the Bjorken limit (large Q^2), the QCD factorization theorem for DVCS and HEMP on any hadronic target [13,14] states that corresponding scattering amplitudes factorize in convolution of perturbative (hard) coefficient functions with nonperturbative (soft) matrix elements, which are parameterized in terms of generalized parton distributions (GPDs). GPDs are universal (process-independent) functions that contain information on parton distributions and correlations in hadrons and in matrix elements describing transitions between different hadrons (see above).

In this paper, we consider DVCS on nuclear targets, $\gamma^* A \to \gamma A$, which gives an access to nuclear GPDs. We would like to single out the following three important roles of nuclear DVCS:

(i) It gives information on nucleon GPDs, which is complimentary to that obtained in DVCS on the free proton;
(ii) It allows us to study novel nuclear effects, which decouple from DIS and elastic scattering on nuclei;
(iii) It imposes stringent constraints on theoretical models attempting to give a covariant description of the nuclear structure.

In this paper, we deal with the first point. In particular, we examine the role of the neutron contribution to nuclear DVCS asymmetries on a wide range of nuclei. This allows one to constrain neutron GPDs, which are not directly accessible.

Nuclear DVCS opens possibilities to study novel nuclear effects, which seem to be predominantly encoded in the real part of the DVCS scattering amplitude. It was speculated in the framework of the nuclear liquid drop model that the so-called nuclear D-term, which contributes to the real part of the nuclear DVCS amplitude, has a fast, nontrivial dependence on the atomic number A ($A^{7/3}$ vs naively expected A^2) [23]. This observation was confirmed by an analysis of nuclear GPDs using the Walecka model [24]. In that analysis, the fast A-dependence of nuclear GPDs comes from nuclear meson degrees of freedom. Hence, the measurement of DVCS observables sensitive to the real part of the DVCS amplitude gives a possibility to study non-nucleon (mesonic) degrees of freedom in nuclei.

In the small Bjorken x_B limit, a model for nuclear GPDs, which combines the model for nucleon GPDs based on the aligned-jet model with phenomenological parametrizations of usual nuclear PDFs, was suggested in [25,26]. It was found that the ratio of the real parts of the nuclear to nucleon DVCS amplitudes has a very unexpected behavior as a function of x_B, which is very different from the corresponding ratio of the imaginary parts. The latter was found to be similar to the ratio of the nuclear to nucleon structure functions measured in inclusive DIS. This, again, hints that novel nuclear effects might be lurking in the real part of the nuclear DVCS amplitude.

The third role of nuclear DVCS is related to the fact that nuclear GPDs, similarly to nucleon GPDs, should obey the fundamental properties of polynomiality and positivity. In order to achieve these properties, theoretical models used to build nuclear GPDs must give a covariant description of the nuclear structure, which imposes severe constraints on the

*vguzey@jlab.org; http://www.jlab.org/vguzey

nuclear models. This problem was discussed in relation to modeling deuteron GPDs in [27].

GPDs of composite hadrons (nucleons and pions), which satisfy the properties of polynomiality and positivity, were modeled using the representation of GPDs essentially in terms of a triangle Feynman diagram [28–32]. In principle, this approach can be extended to nuclear targets. However, it appears very difficult to build a successful phenomenology of nuclear GPDs based on triangle Feynman diagrams, which would make a connection with the quantities used for the description of the nuclear structure in traditional nuclear physics such as, e.g., the nuclear spectral function and the binding energy.

The literature on nuclear DVCS and nuclear GPDs is not numerous and can readily be comprehensively reviewed.

Originally, the formalism of deuteron GPDs was developed in [33]. The formalism of nuclear GPDs of any spin-0, spin-1/2, and spin-1 nuclei was presented in [34]. Assuming that nuclei are collections of free protons and neutrons, predictions for DVCS observables (asymmetries) were made. In particular, in accord with the earlier result of [35], it was predicted that the nuclear DVCS beam-spin asymmetry is enhanced compared to the free proton asymmetry, $A_{\rm LU}^A(\phi)/A_{\rm LU}^p(\phi) \sim 5/3$, for spin-0 and spin-1/2 nuclei.

Up until now, the main theoretical approach to dynamical models of nuclear GPDs was the convolution approximation, which assumes that nuclear GPDs are given by convolution of unmodified or modified nucleon GPDs with the distribution of nucleons in the nuclear target. The latter distribution is obtained from the nonrelativistic nuclear wave function. Within the convolution approximation, GPDs were considered of such nuclei as deuterium [27,36,37], ^{3}He [38,39], ^{4}He [40,41], ^{20}Ne, and ^{76}Kr [35], a wide range of nuclei from ^{12}C to ^{208}Pb [24] (in that analysis, besides nucleons, meson degrees of freedom were also used in the convolution).

While the convolution approximation is reliable for $x_B > 0.1$, it is not applicable for small x_B, where such coherent nuclear effects as nuclear shadowing and antishadowing become important. A model of nuclear GPDs for heavy nuclei, which takes into account nuclear shadowing and antishadowing, was proposed in [25,26] (see also the discussion above).

Another important aspect of nuclear DVCS, at least from the practical point of view, is the interplay between the coherent (the nucleus remains intact) and incoherent (the nucleus excites or breaks up) contributions to nuclear DVCS. This was studied in [35] and a general expression for nuclear DVCS asymmetries, which interpolates between the coherent and incoherent regimes, was derived. It was predicted that for the coherent contribution, in the kinematics of the HERMES experiment, the ratio of the nuclear (^{20}Ne and ^{76}Kr) to the free proton beam-spin asymmetries is enhanced, $A_{\rm LU}^A(\phi)/A_{\rm LU}^p(\phi) \approx 1.8$. For the incoherent contribution, it was predicted that $A_{\rm LU}^A(\phi)/A_{\rm LU}^p(\phi) = 1$, provided that the neutron contribution to the nuclear DVCS amplitude was neglected.

It is the main goal of the present work to go beyond this approximation and to study the role of the neutron contribution in coherent and incoherent nuclear DVCS observables (asymmetries).

On the experimental side, initial measurements of nuclear DVCS were reported by the HERMES collaboration at DESY [42] and more data on nuclear DVCS at HERMES is expected [43]. The Hall A collaboration at Jefferson Lab recently reported a measurement of DVCS on deuterium with the aim to study the neutron GPDs [44]. It is planned that nuclear GPDs will be studied at Jefferson Lab at the present 6 GeV and the future 12 GeV energy of the electron beam. At high energies, nuclear GPDs will be studied at the LHC in ultraperipheral nucleus-nucleus collisions, see, e.g., [45], and at the future Electron-Ion Collider.

This paper is organized as follows. In Sec. II, we explain our model of nuclear GPDs. The interpolating formula between the coherent and incoherent regimes of nuclear DVCS is derived in Sec. III. Predictions for the nuclear beam-spin DVCS asymmetry in HERMES and JLab kinematics, with an emphasis on the neutron contribution, are presented in Sec. IV. We summarize and discuss our results in Sec. V.

II. MODEL FOR NUCLEAR AND NUCLEON GPDs

We use a simple model for nuclear GPDs that captures main features of the dependence of nuclear GPDs on the atomic number A and on the momentum transfer t. We assume that the nucleus consists of A uncorrelated nucleons: Z protons and $N = A - Z$ neutrons [34], see Fig. 1. For simplicity, we shall consider spin-0 nuclei. In this case, there is only one leading-twist quark nuclear GPD, H_A^q, which can be expressed

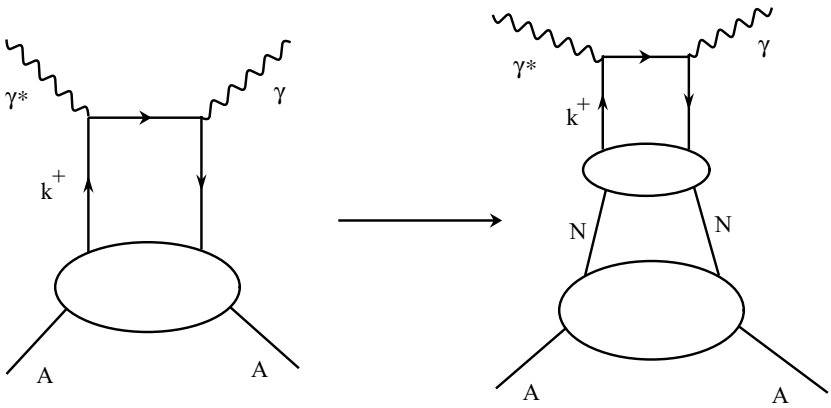

FIG. 1. Schematic representation of nuclear quark GPDs.

in terms of the free proton and neutron quark GPDs H^q and E^q as follows:

$$H_A^q(x,\xi_A,Q^2,t) = \left|\frac{dx_N}{dx}\right| \Bigg[Z \left(H^{q/p}(x_N,\xi_N,Q^2,t) + \frac{t}{4m_N^2} E^{q/p}(x_N,\xi_N,Q^2,t) \right) + N \left(H^{q/n}(x_N,\xi_N,Q^2,t) + \frac{t}{4m_N^2} E^{q/n}(x_N,\xi_N,Q^2,t) \right) \Bigg] F_A(t), \tag{1}$$

where $F_A(t)$ is the nuclear form factor normalized to unity; m_N is the nucleon mass; other variables are introduced below. Note that the GPDs H^q and E^q enter Eq. (1) in the combination that leads to the proper nuclear charge form factor [35].

The Bjorken variable x_A is defined with respect to the nuclear target. In the laboratory frame, we have

$$x_A = \frac{Q^2}{2\nu M_A} = \frac{Q^2}{2\nu A m_N} = \frac{1}{A}\, x_B, \tag{2}$$

where ν is the photon energy; M_A is the mass of the nucleus. From the relations

$$\xi_A = \frac{x_A}{2-x_A}, \quad \xi_N = \frac{x_B}{2-x_B}, \tag{3}$$

it follows that

$$\frac{\xi_N}{1+\xi_N} = A \frac{\xi_A}{1+\xi_A}. \tag{4}$$

Next we find the relation between x and x_N. In the symmetric notation [8], the outgoing interacting quark carries the plus-momentum $k^+ = (x+\xi_A)\bar{P}_A^+$, see the left-hand side of Fig. 1. On the other hand, k^+ can also be written as (see the right-hand side of Fig. 1)

$$k^+ = (x_N+\xi_N)\bar{P}_N^+ = (x_N+\xi_N)\left(\frac{1}{A}P_A^+ + \frac{\Delta^+}{2}\right) = (x_N+\xi_N)\left(\frac{1}{A}(1+\xi_A) - \xi_A\right)\bar{P}_A^+. \tag{5}$$

In this derivation, we used the assumption that $P_N^+ = P_A^+/A$. Therefore, with the help of Eq. (4), we find that

$$\frac{x_N}{x} = \frac{\xi_N}{\xi_A}. \tag{6}$$

In the forward limit, Eq. (1) reduces to the model for nuclear quark parton distribution functions (PDFs),

$$q_A(x_A,Q^2) = A[Z\, q_p(x_B,Q^2) + N\, q_n(x_B,Q^2)]. \tag{7}$$

These nuclear PDFs satisfy the baryon number (total charge) and momentum sum rules,

$$\int_{-1}^{1} dx_A \sum_q e_q\, q_A(x_A,Q^2) = \int_{-1}^{1} dx_B \sum_q e_q [Z\, q_p(x_B,Q^2) + N\, q_n(x_B,Q^2)] = Z,$$

$$\int_{-1}^{1} dx_A \sum_q x_A q_A(x_A,Q^2) = \int_{-1}^{1} dx_B \sum_q x_B \left[\frac{Z}{A}\, q_p(x_B,Q^2) + \frac{N}{A}\, q_n(x_B,Q^2)\right]. \tag{8}$$

Taking the first x-moment of the nuclear GPD weighted with quark charges, one obtains the nuclear electric form factor,

$$F_A^{e.m.}(t) \equiv \int_{-1}^{1} dx \sum_q e_q\, H_A^q(x,\xi_A,Q^2,t) = \left[Z F_E^p(t) + N F_E^n(t)\right] F_A(t), \tag{9}$$

where $F_E^{p,n}(t) = F_1^{p,n}(t) + t/(4m_N^2) F_2^{p,n}(t)$ are the electric form factors of the proton and neutron expressed in terms of the corresponding Dirac and Pauli form factors.

The fact that the right-hand side of Eq. (9) does not depend on ξ_A means that the first x-moment of H_A^q satisfies polynomiality. An examination shows that higher x-moments of H_A^q do not satisfy polynomiality, even if the proton and neutron GPDs do. As we mentioned in the Introduction, it is an outstanding theoretical challenge to build a model of nuclear GPDs with the property of polynomiality (and positivity), which would make a connection to the quantities used for the description of the nuclear structure in traditional nuclear physics such as, e.g., the nuclear spectral function and the binding energy.

DVCS observables are expressed in terms of the so-called Compton form factors (CFFs), which are defined as nuclear GPDs convoluted with the corresponding hard scattering coefficients. For spin-0 nuclei, to the leading order in α_s, the only CFF reads

$$\begin{aligned}
&\mathcal{H}_A(\xi_A,Q^2,t) \\
&= \sum e_q^2 \int_{-1}^{1} dx\, H_A^q(x,\xi_A,Q^2,t) \times \left(\frac{1}{x-\xi_A+i0} + \frac{1}{x+\xi_A-i0}\right) \\
&= \left(\frac{\xi_N}{\xi_A}\right) \sum e_q^2 \int_{-1}^{1} dx_N \Bigg[Z \left(H^{q/p}(x_N,\xi_N,Q^2,t) + \frac{t}{4m_N^2} E^{q/p}(x_N,\xi_N,Q^2,t) \right) + N \left(H^{q/n}(x_N,\xi_N,Q^2,t) + \frac{t}{4m_N^2} E^{q/n}(x_N,\xi_N,Q^2,t) \right) \Bigg] \\
&\quad \times F_A(t) \left(\frac{1}{x_N-\xi_N+i0} + \frac{1}{x_N+\xi_N-i0}\right) \\
&= \left(\frac{\xi_N}{\xi_A}\right) \left[Z \left(\mathcal{H}^p(\xi_N,Q^2,t) + \frac{t}{4m_N^2} \mathcal{E}^p(\xi_N,Q^2,t) \right) + N \left(\mathcal{H}^n(\xi_N,Q^2,t) + \frac{t}{4m_N^2} \mathcal{E}^n(\xi_N,Q^2,t) \right) \right] F_A(t).
\end{aligned} \tag{10}$$

An important corollary of Eq. (10) is that $\mathcal{H}_A$ scales as A^2.

In our analysis, for the nucleon CFFs $\mathcal{H}^{p,n}$ and $\mathcal{E}^{p,n}$, we used results of the minimal model of the dual parametrization of nucleon GPDs [46]. The name "dual" is a reflection of the fact that the parametrization is given as an infinite series of generalized light-cone distribution amplitudes in the t-channel [47], which is similar to the construction of scattering amplitudes using the assumption of duality in hadronic physics.

The minimal model of the dual parametrization is designed primarily for not very large values of Bjorken x_B, where the model can be formulated in terms of the usual parton distributions, the forward limit of the GPD $E^{q/p}$ and Gegenbauer moments of the nucleon D-term. Assuming a nonfactorized Regge-motivated t-dependence and adjusting the slopes of Regge trajectories, the resulting model leads to a good description of high-energy (small-x_B) H1 and ZEUS data on the DVCS cross section, HERMES data on various DVCS asymmetries and the early 2001 CLAS data on the beam-spin DVCS asymmetry [46].

Naturally, the minimal model of the dual parametrization has its limitations, especially when applied to moderate values of x_B. Difficulties of the dual parametrization in the description of the recent high precision Jefferson Lab (Hall A) data on the DVCS cross section were discussed in [48].

We give our numerical predictions in the form of ratios of nuclear to free proton DVCS asymmetries. Thus, we expect that the intrinsic dependence on the particular model of nucleon GPDs will partially cancel in the ratio.

In the present numerical analysis, the role of the GPD $E^{q/p}$ is not important. Our predictions are not sensitive to the assumption about the proton total angular momentum carried by quarks, J_u and J_d: We simply set $J_u = J_d = 0$.

For the nuclear form factor $F_A(t)$, for ^{4}He, we used the result of [49]. For other nuclei, we used the parametrization of nuclear charge density distributions [50] (see Appendix for details).

III. COHERENT AND INCOHERENT NUCLEAR DVCS

In the situation, when the recoiled nucleus is not detected, measurements of DVCS observables with nuclear targets necessarily involve the coherent and incoherent contributions [35]. The former contribution corresponds to the case when the nuclear target stays intact, and it dominates at small values of the momentum transfer t. The latter contribution corresponds to the case when the initial nucleus A transforms into the system of $A-1$ spectator nucleons (bound or free) and one interacting nucleon, and it dominates at large t. In the approximation of closure over the final nuclear states, the exact structure of the final system of $A-1$ nucleons is not important. The coherent DVCS and BH amplitudes (one of two possible attachments of the real photon to the lepton lines is shown) are presented in Fig. 2; the incoherent DVCS and BH amplitudes are shown in Fig. 3.

In order to correctly sum the coherent and incoherent contributions to the $eA \to e\gamma A$ cross section, let us schematically

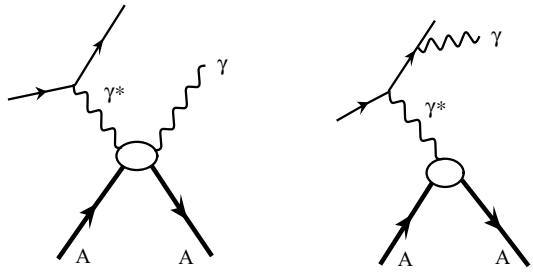

FIG. 2. The coherent DVCS (left) and Bethe-Heitler (right) scattering amplitudes on a nucleus A. Only one of two possible BH amplitudes is shown.

write the corresponding amplitude as, see, e.g., [51],

$$\mathcal{A}(t) = \langle A^*| \sum_i^A J_i\, e^{i\vec{\Delta}\cdot\vec{r}_i} |A\rangle, \tag{11}$$

where A^* represents the final state consisting of A nucleons (coherently scattered nucleus or any product of the nuclear dissociation); J_i represents the operator corresponding to the interaction with the nucleon i (one-particle operator); the summation runs over all nucleons of the target; $\vec{\Delta}$ is the momentum transfer. Assuming that the states $|A^*\rangle$ form a complete set, the cross section summed over the nuclear final states can be expressed in the following form:

$$\begin{aligned}
\frac{d\sigma_A}{dt} &\propto \sum_{A^*} \langle A| \sum_j^A J_j^\dagger\, e^{-i\vec{\Delta}\cdot\vec{r}_j} |A^*\rangle \langle A^*| \sum_i^A J_i\, e^{i\vec{\Delta}\cdot\vec{r}_i} |A\rangle \\
&= \langle A| \sum_{i,j}^A J_j^\dagger J_i\, e^{i\vec{\Delta}\cdot(\vec{r}_i - \vec{r}_j)} |A\rangle \\
&= \langle A| \sum_{i\neq j}^A J_j^\dagger J_i\, e^{i\vec{\Delta}\cdot(\vec{r}_i - \vec{r}_j)} |A\rangle + \langle A| \sum_i^A J_i^\dagger J_i |A\rangle \\
&\approx A(A-1)\langle A| J_N^\dagger J_N\, e^{i\vec{\Delta}\cdot(\vec{r}_i - \vec{r}_j)} |A\rangle + A\,\langle N| J_N^\dagger J_N |N\rangle \\
&\propto A(A-1) F_A^2(t') \frac{d\tilde{\sigma}_N}{dt} + A\,\frac{d\sigma_N}{dt},
\end{aligned} \tag{12}$$

where $d\tilde{\sigma}_N/dt$ is the scattering cross section on the bound nucleon; $d\sigma_N/dt$ corresponds to the quasifree nucleon; $t' = A/(A-1)\,t$ [51]. For the sake of the argument, we did

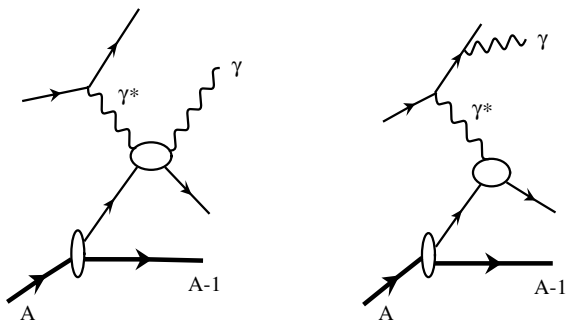

FIG. 3. The incoherent DVCS and Bethe-Heitler scattering amplitudes. The initial nucleus A transforms into a final state containing $A-1$ spectator nucleons (free or bound) and an interacting nucleon.

not distinguish between protons and neutrons. Adopting the HERMES terminology, we shall call the first term in the last line of Eq. (12) *coherent-enriched* [43]. The second term is the incoherent contribution.

The dependence of the coherent-enriched contribution on t is steep and is governed by the nuclear form factor squared $F_A^2(t')$. Therefore, this contribution dominates the nuclear cross section at small t. The t-dependence of the incoherent contribution is much slower and is determined by the t-dependence of the cross section on quasifree nucleons $d\sigma_N/dt$. While this contribution is present at all t, it dominates the nuclear cross section at large t.

Besides the t-dependence, the coherent-enriched and incoherent contributions have different A-dependences. The coherent-enriched contribution scales as $A(A-1)$; the incoherent contribution scales as A.

Let us now consider the case when the recoiled nucleus is intact. In this case, $|A^*\rangle = |A\rangle$ in Eq. (11), and the expression for the $eA \to e\gamma A$ cross section becomes

$$\frac{d\sigma_A}{dt} = A^2 F_A^2(t) \frac{d\tilde{\sigma}_N}{dt}. \tag{13}$$

In Eq. (13), $d\sigma_A/dt$ is the genuine coherent nuclear scattering cross section, which scales as A^2 and whose t-dependence is steep and is given by the nuclear form factor squared $F_A^2(t)$.

Using Eq. (12), the full-fledged differential cross section for the $eA \to e\gamma A$ reaction [10] can be written as a sum of the coherent-enriched and incoherent contributions,

$$\frac{d\sigma_A}{dx_A\, dy\, dt\, d\phi} = \frac{\alpha^3 x_A y}{8\pi Q^2 \sqrt{1+\epsilon^2}} \left(\frac{A-1}{A} \left| \frac{\mathcal{T}_A(x_A, y)}{e^3} \right|^2 + \left(\frac{x_B}{x_A}\right)^2 \sum_{i=1}^{A} \left| \frac{\mathcal{T}_i(x_B, y)}{e^3} \right|^2 \right), \tag{14}$$

where $\mathcal{T}_A$ is the amplitude for the coherent $eA \to e\gamma A$ scattering; $\mathcal{T}_i$ are the amplitudes for quasifree incoherent $eA \to e\gamma A$ scattering; the $(A-1)/A$ factor originates from Eq. (12); the $(x_B/x_A)^2$ factor is required for the incoherent contribution not to depend on A; ϕ is the angle between the lepton scattering and the production planes.

It is important to note that the prefactor $(A-1)/A$ corresponds to the DVCS amplitude squared and to the interference between the DVCS and Bethe-Heitler (BH) amplitudes. For the BH amplitude squared, $(A-1)/A$ should be replaced by $(Z-1)/Z$.

In Eq. (14), in the laboratory frame,

$$y = \frac{\nu}{E}, \quad \epsilon = 2\frac{x_A M_A}{Q} = 2\frac{x_B m_N}{Q}, \tag{15}$$

where E is the energy (momentum) of the incoming lepton. Note that the variables y, ϵ and t are the same for nuclear and nucleon targets.

For the comparison with the free nucleon case and with experiments, it is convenient to express σ_A as a function of x_B,

$$\frac{d\sigma_A}{dx_B\, dy\, dt\, d\phi} = \frac{\alpha^3 x_B y}{8\pi Q^2 \sqrt{1+\epsilon^2}} \left(\frac{A-1}{A^3} \left| \frac{\mathcal{T}_A(x_A, y)}{e^3} \right|^2 + \sum_{i=1}^{A} \left| \frac{\mathcal{T}_i(x_B, y)}{e^3} \right|^2 \right). \tag{16}$$

For the BH amplitude squared, $(A-1)/A^3$ should be replaced by $(Z-1)/(ZA^2)$.

For illustration, let us consider the DVCS contribution to Eq. (16). In this case, $|\mathcal{T}_A|^2 \propto |\mathcal{H}_A|^2$, which scales as $[A^2 F_A(t')]^2$, see Eq. (10). Therefore, the first term in Eq. (16) behaves as $A^2 F_A^2(t')$. The second term has the t-dependence determined by the nucleon GPDs and scales as A.

In the situation where the recoiled nucleus is detected, the $eA \to e\gamma A$ cross section is purely coherent, and it reads

$$\frac{d\sigma_A}{dx_B\, dy\, dt\, d\phi} = \frac{\alpha^3 x_B y}{8\pi Q^2 \sqrt{1+\epsilon^2}} \frac{1}{A^2} \left| \frac{\mathcal{T}_A(x_A, y)}{e^3} \right|^2. \tag{17}$$

IV. NUCLEAR DVCS ASYMMETRIES

In this section, as an example of DVCS asymmetries, we consider the beam-spin nuclear DVCS asymmetry in the presence of the coherent and incoherent contributions, with an emphasis on the neutron contribution. We make predictions relevant for the HERMES and JLab kinematics.

A. Coherent and incoherent contributions to DVCS asymmetries

Expressions for nuclear DVCS asymmetries can be readily obtained from Eqs. (16) and (17). In this work, we consider the beam-spin asymmetry, $A_{\rm LU}$, which is measured with the longitudinally-polarized lepton beam and the unpolarized target.

The nuclear and nucleon amplitudes squared in Eqs. (16) and (17) receive contributions from the DVCS and Bethe-Heitler (BH) scattering amplitudes and their interference,

$$|\mathcal{T}|^2 = |\mathcal{T}_{\rm DVCS}|^2 + |\mathcal{T}_{\rm BH}|^2 + \mathcal{I}, \tag{18}$$

where $\mathcal{I} = \mathcal{T}^*_{\rm DVCS}\mathcal{T}_{\rm BH} + \mathcal{T}^*_{\rm BH}\mathcal{T}_{\rm DVCS}$.

The expression for the nuclear DVCS beam-spin asymmetry reads [10]

$$A^A_{\rm LU}(\phi) = \frac{\Delta\mathcal{I}}{|\mathcal{T}_{\rm BH}|^2 + \mathcal{I} + |\mathcal{T}_{\rm DVCS}|^2}, \tag{19}$$

where $\Delta\mathcal{I} = 1/2(\mathcal{I}^{\lambda=1} - \mathcal{I}^{\lambda=-1})$ with λ the helicity of the incoming lepton; all other contributions correspond to the unpolarized beam.

It is important to note that we work in the leading twist (twist-two) approximation. Therefore, the numerator of Eq. (19) does not contain the twist-three contribution of the DVCS amplitude squared, and $\Delta\mathcal{I}$, $\mathcal{I}$ and $|\mathcal{T}_{\rm DVCS}|^2$ are evaluated at the twist-two accuracy (see Appendix for details).

In the situation corresponding to Eq. (16), each term in Eq. (19) contains the coherent-enriched and incoherent

contributions,

$$\mathcal{I} = \frac{A-1}{A^3}\mathcal{I}^A + Z\mathcal{I}^p + N\,\mathcal{I}^n,$$
$$|\mathcal{T}_{\rm BH}|^2 = \frac{Z-1}{ZA^2}\left|\mathcal{T}^A_{\rm BH}\right|^2 + Z\left|\mathcal{T}^p_{\rm BH}\right|^2 + N\left|\mathcal{T}^n_{\rm BH}\right|^2, \qquad (20)$$
$$|\mathcal{T}_{\rm DVCS}|^2 = \frac{A-1}{A^3}\left|\mathcal{T}^A_{\rm DVCS}\right|^2 + Z\left|\mathcal{T}^p_{\rm DVCS}\right|^2 + N\left|\mathcal{T}^n_{\rm DVCS}\right|^2.$$

Expressions for the free nucleon contributions $\mathcal{I}^{p,n}$, $|\mathcal{T}^{p,n}_{\rm BH}|^2$, and $|\mathcal{T}^{p,n}_{\rm DVCS}|^2$ in terms of $\cos\phi$ and $\sin\phi$-harmonics are derived in [10]. As a model of the nucleon GPDs, we used the results of the dual parametrization of nucleon GPDs with $J_u = J_d = 0$ [46].

Expressions for $\mathcal{I}^A$, $|\mathcal{T}^A_{\rm BH}|^2$, and $|\mathcal{T}^A_{\rm DVCS}|^2$ for spin-0 zero nuclei are the same as for the pion [53], after the replacement of the pion charge form factor by the nuclear one evaluated at $t' = A/(A-1)t$.

In the case of the purely coherent scattering corresponding to Eq. (17), the terms in Eq. (20) should be replaced by the following expressions:

$$\mathcal{I} = \frac{1}{A^2}\mathcal{I}^A,$$
$$|\mathcal{T}_{\rm BH}|^2 = \frac{1}{A^2}\left|\mathcal{T}^A_{\rm BH}\right|^2, \qquad (21)$$
$$|\mathcal{T}_{\rm DVCS}|^2 = \frac{1}{A^2}\left|\mathcal{T}^A_{\rm DVCS}\right|^2.$$

In the purely coherent case, the nuclear form factor is evaluated at the momentum transfer t.

Using Eqs. (19), (20), and (21), one can qualitatively estimate the behavior of $A^A_{\rm LU}(\phi)$ as a function of A and Z. Provided the $|\mathcal{T}_{\rm BH}|^2$-term dominates the unpolarized cross section, the coherent-enriched contribution to $A^A_{\rm LU}(\phi)$ scales as $(A-1)/(Z-1)$. The purely coherent $A^A_{\rm LU}(\phi)$ scales as A/Z.

All expressions used in Eqs. (20) and (21) are collected in the Appendix.

We would like to point out that $\mathcal{I}^A$ and $|\mathcal{T}^A_{\rm DVCS}|$ in the right-hand side of Eq. (20) involve the nuclear CFF $\mathcal{H}_A$ proportional to the proton and neutron contributions, which scale as Z and N, respectively. In the case of the coherent-enriched contribution, the relative weight of the proton and neutron contributions is slightly different, which matters only for light nuclei such ^{4}He and ^{14}N. However, even for the light nuclei, this has a negligibly small effect on our numerical predictions.

B. Nuclear DVCS beam-spin asymmetry $A_{\rm LU}$ in HERMES kinematics

In the measurement of nuclear DVCS at HERMES, the recoiled nucleus is not detected, but reconstructed using the missing mass technique [42,43]. This corresponds to the situation, when one sums over all final nuclear states. This means that the nuclear beam-spin DVCS asymmetry, $A^A_{\rm LU}$, receives contribution from the coherent-enriched and incoherent terms and is given by Eqs. (19) and (20).

We quantify our numerical predictions for $A^A_{\rm LU}$ by considering the ratio of the nuclear to the free proton asymmetries, $A^A_{\rm LU}(\phi)/A^p_{\rm LU}(\phi)$. This ratio is presented in Fig. 4 as a function of t at an average HERMES kinematic point $x_B = 0.065$ and $Q^2 = 1.7$ GeV^2 [43]. The asymmetries are evaluated at $\phi = 90^\circ$. Different curves correspond to different nuclei: ^{4}He, ^{14}N, ^{20}Ne, ^{84}Kr, and ^{131}Xe.

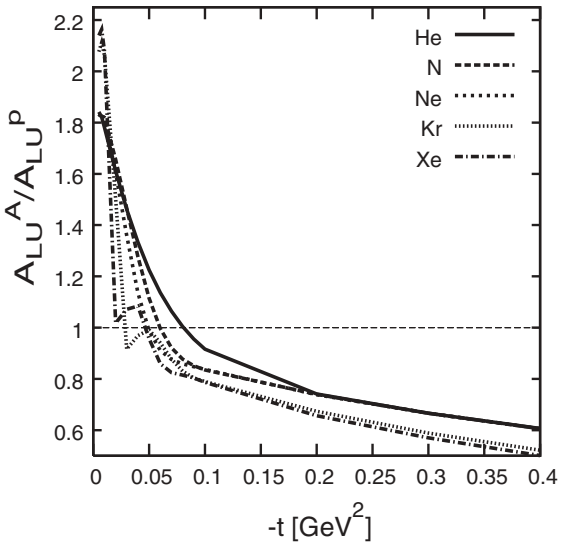

FIG. 4. The ratio of the nuclear to free proton beam-spin DVCS asymmetries, $A^A_{\rm LU}(\phi)/A^p_{\rm LU}(\phi)$, as a function of the momentum transfer t for He, N, Ne, Kr, and Xe nuclei. The calculation is done at $x_B = 0.065$, $Q^2 = 1.7$ GeV^2 [43], and $\phi = 90^\circ$.

At small values of t, when the nuclear asymmetries (cross sections) are dominated by the coherent-enriched contribution, $A^A_{\rm LU}/(\phi)A^p_{\rm LU}(\phi) = 1.8$–$2.2$, which is consistent with the previous analyses [34,35]. The enhancement of $A^A_{\rm LU}(\phi)/A^p_{\rm LU}(\phi)$ above unity is the combinatoric effect: Since the interference between the Bethe-Heitler and the DVCS amplitudes scales as $Z(A-1)$ and the Bethe-Heitler amplitude squared scales as $Z(Z-1)$, $A^A_{\rm LU}(\phi)$ scales as $(A-1)/(Z-1)$.

At large values of t, when the nuclear form factor eliminates the coherent-enriched term, $A^A_{\rm LU}(\phi)$ is given by the incoherent contribution, and $A^A_{\rm LU}(\phi)/A^p_{\rm LU}(\phi) < 1$.

The fact that $A^A_{\rm LU}(\phi)/A^p_{\rm LU}(\phi) < 1$ is a result of the neutron contribution to $A^A_{\rm LU}(\phi)$, see Eq. (20). First (this is effect is largest), the neutron contribution decreases the numerator of $A^A_{\rm LU}(\phi)$, since $F_{1n} < 0$, while $F_{1p} > 0$. Second, the positive neutron contributions $|\mathcal{T}^n_{\rm BH}|^2 + \mathcal{I}^n$ (somewhat suppressed by the neutron electromagnetic form factors compared to the proton contribution) and $|\mathcal{T}^n_{\rm DVCS}|^2$ (similar to the proton contribution) increase the denominator of $A^A_{\rm LU}(\phi)$. The decrease of the numerator of $A^A_{\rm LU}(\phi)$ and the increase of the denominator work together to reduce $A^A_{\rm LU}(\phi)/A^p_{\rm LU}(\phi)$ significantly below unity at large t.

Note that our present finding that $A^A_{\rm LU}(\phi)/A^p_{\rm LU}(\phi) < 1$ at large t does not contradict the original analysis [35]. In that work, it was predicted that $A^A_{\rm LU}(\phi)/A^p_{\rm LU}(\phi) \to 1$ as t becomes large, if the neutron contribution to the nuclear asymmetry is neglected. In the present work, we went beyond this approximation and found that the neutron contribution is not negligible and leads to $A^A_{\rm LU}(\phi)/A^p_{\rm LU}(\phi) < 1$. Therefore, studies of the incoherent contribution to nuclear DVCS

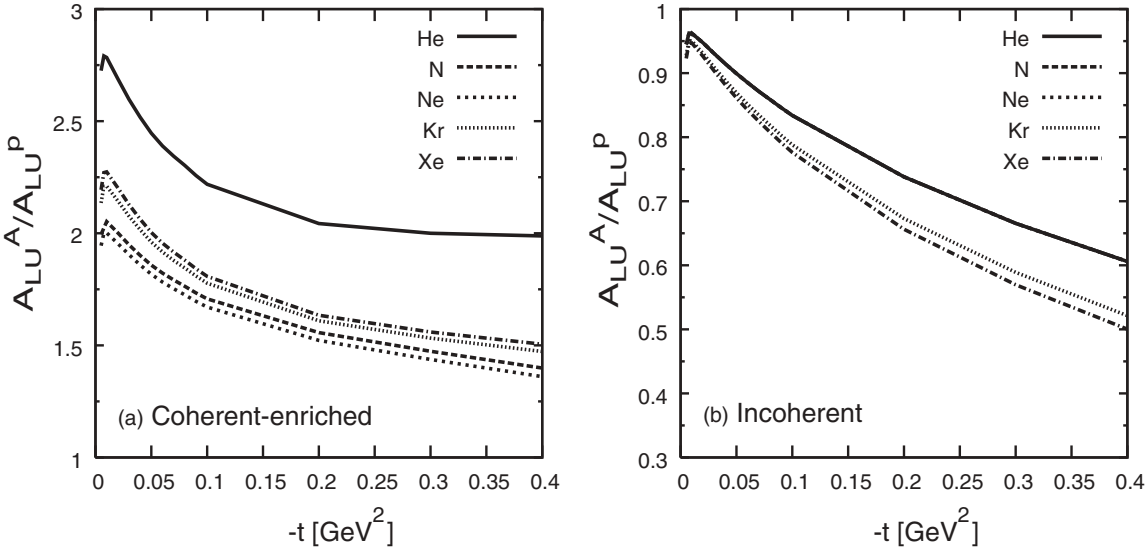

FIG. 5. The ratio of the nuclear to free proton beam-spin DVCS asymmetries, $A_{\rm LU}^A(\phi)/A_{\rm LU}^p(\phi)$, as a function of the momentum transfer t for He, N, Ne, Kr, and Xe nuclei. The calculation is done at $x_B = 0.065$, $Q^2 = 1.7\ \text{GeV}^2$ [43] and $\phi = 90^\circ$. (a) corresponds to the coherent-enriched contribution; (b) corresponds to the incoherent contribution.

asymmetries is a sensitive tool to constrain neutron GPDs. The Hall A collaboration at Jefferson Lab explored this possibility using the deuterium target [44].

Note also that the neutron GPDs enter the model of nuclear GPDs, see Eq. (1). Hence, nuclear DVCS observables in the coherent regime also provide certain constraints for the neutron GPDs, albeit those constraints are less stringent and more model-dependent compared to the incoherent regime.

By studying the t-dependence of the nuclear DVCS cross section, the HERMES analysis separated the coherent-enriched and incoherent contributions to $A_{\rm LU}^A(\phi)$. Our predictions for these two contributions are presented separately in Fig. 5. The left panel corresponds to the coherent-enriched contribution to $A_{\rm LU}^A(\phi)$, which was calculated keeping only the first terms in Eq. (20). The right panel corresponds to the incoherent contribution calculated using the last two terms in Eq. (20).

In the left panel of Fig. 5, the curve for ^{4}He lies above the curves for other nuclei because the coherent-enriched contribution scales $(A-1)/(Z-1)$.

In the right panel of Fig. 5, the ratio $A_{\rm LU}^A(\phi)/A_{\rm LU}^p(\phi)$ at small t is close to unity because the neutron contribution is suppressed by the small value of the neutron Dirac form factor $F_{1n}(t)$. As $|F_{1n}(t)|$ increases with increasing $|t|$, the ratio $A_{\rm LU}^A(\phi)/A_{\rm LU}^p(\phi)$ begins to progressively deviate from unity.

Taking different t-slices of Fig. 4, we can study the A-dependence of $A_{\rm LU}^A(\phi)$. Figure 6 presents $A_{\rm LU}^A(\phi)/A_{\rm LU}^p(\phi)$ as a function of A at $t = -0.018\ \text{GeV}^2$ (upper set of points) and $t = -0.2\ \text{GeV}^2$ (lower set of points). These two values of t correspond to the average HERMES values [43].

The interpretation of Fig. 6 is the same as for Fig. 4. At small values of t, the coherent-enriched contribution dominates and $A_{\rm LU}^A(\phi)/A_{\rm LU}^p(\phi) > 1$ due to the fact that $A_{\rm LU}^A(\phi)$ scales roughly as $(A-1)/(Z-1)$. At large t, where only the incoherent contribution matters, $A_{\rm LU}^A(\phi)/A_{\rm LU}^p(\phi) < 1$ due to the neutron contribution (see the discussion above).

Results presented in Fig. 6 should be compared to the results of the HERMES analysis [43]. At $t = -0.018\ \text{GeV}^2$, the agreement between our calculations (the upper set of points) and the HERMES data is excellent. For the nuclei of ^{4}He, ^{14}N, ^{20}Ne, and ^{84}Kr, $A_{\rm LU}^A(\phi)/A_{\rm LU}^p(\phi) \approx 1.65$. For the nucleus of ^{131}Xe, $A_{\rm LU}^A(\phi)/A_{\rm LU}^p(\phi) = 1.23$, which is smaller than for other lighter nuclei because of the reduction of the coherent-enriched contribution by the nuclear form factor.

At $t = -0.2\ \text{GeV}^2$, we predict that $A_{\rm LU}^A(\phi)/A_{\rm LU}^p(\phi) = 0.66$–$0.74$, depending of the target nucleus. The experimental

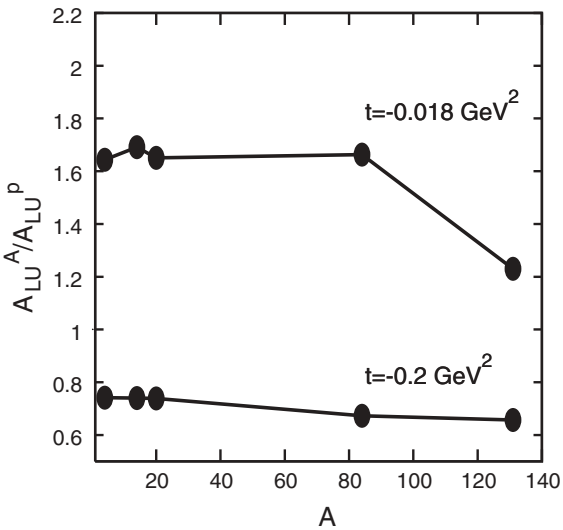

FIG. 6. The ratio of the nuclear to free proton beam-spin DVCS asymmetries, $A_{\rm LU}^A(\phi)/A_{\rm LU}^p(\phi)$, as a function of A. The calculation is done at $x_B = 0.065$, $Q^2 = 1.7\ \text{GeV}^2$ and $\phi = 90^\circ$.

uncertainties of the HERMES data are too large and, in general, do not exclude the deviation of $A_{\rm LU}^A(\phi)/A_{\rm LU}^p(\phi)$ from unity, as we predict.

C. Nuclear DVCS beam-spin asymmetry $A_{\rm LU}$ in Jefferson Lab kinematics

There exists an exciting possibility to study purely coherent nuclear DVCS at Jefferson Lab using the BoNuS recoil detector. In particular, an experiment to study $A_{\rm LU}$ in coherent and incoherent DVCS on ^{4}He has been proposed [52]. The main advantages of the proposed experiment compared to HERMES are exclusivity of the measurement, which will allow to measure the purely coherent DVCS, and small projected errors due to high statistics, which will enable one to unambiguously determine the magnitude of $A_{\rm LU}$ in the coherent and incoherent regimes. In addition, the proposed experiment might shed some light on the question of modifications of nucleon GPDs in nuclear medium.

Figure 7 presents our predictions for the ratio of the coherent ^{4}He to free proton beam-spin DVCS asymmetries, $A_{\rm LU}^A(\phi)/A_{\rm LU}^p(\phi)$, as a function of the momentum transfer t. The calculation corresponds to a typical point in the current JLab kinematics: $E = 6\,\text{GeV}, x_B = 0.15$, and $Q^2 = 1.5\,\text{GeV}^2$. The ratio of the asymmetries is evaluated at $\phi = 90^\circ$.

The behavior of $A_{\rm LU}^A(\phi)/A_{\rm LU}^p(\phi)$ presented in Fig. 7 is similar to that in the left-hand side panel of Fig. 5. Since the purely coherent $A_{\rm LU}^A(\phi)$ scales as A/Z, while the coherent-enriched contribution to $A_{\rm LU}^A(\phi)$ scales as $(A-1)/(Z-1)$, the curve in Fig. 7 lies lower than the corresponding curve in the left-hand side of Fig. 5.

In relation to incoherent DVCS on ^{4}He, the proposed experiment at Jefferson Lab will measure the $e^4\text{He} \to epX$ reaction, i.e., DVCS on a quasifree proton. In this case, the neutron contribution is absent and the ratio $A_{\rm LU}^A(\phi)/A_{\rm LU}^p(\phi) =$ 1, provided the bound proton in ^{4}He is not modified. Therefore, this measurement will probe modifications of proton GPDs in ^{4}He.

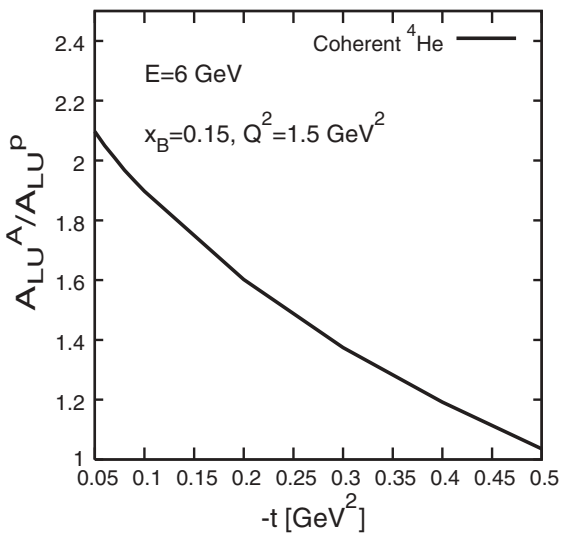

FIG. 7. The ratio of the coherent ^{4}He to free proton beam-spin DVCS asymmetries, $A_{\rm LU}^A(\phi)/A_{\rm LU}^p(\phi)$, as a function of the momentum transfer t. The calculation corresponds to JLab kinematics, $E = 6$ GeV, $x_B = 0.15$, $Q^2 = 1.5\,\text{GeV}^2$, and was performed at $\phi = 90^\circ$.

V. CONCLUSIONS AND DISCUSSION

Using a simple model for nuclear GPDs, we studied the role of the neutron contribution to nuclear DVCS observables. As an example, we used the beam-spin asymmetry $A_{\rm LU}^A$ measured in coherent and incoherent DVCS on a wide range of nuclear targets. In our analysis, we considered the ^{4}He, ^{14}N, ^{20}Ne, ^{84}Kr, and ^{131}Xe nuclei in the HERMES kinematics and the ^{4}He nucleus in the JLab kinematics.

We found that at small values of the momentum transfer t, $A_{\rm LU}^A$ is dominated by the coherent-enriched contribution, which scales as $(A-1)/(Z-1)$. This enhances the nuclear $A_{\rm LU}^A$ compared to the free proton $A_{\rm LU}^p$, $A_{\rm LU}^A(\phi)/A_{\rm LU}^p(\phi) = 1.8$–$2.2$, in accordance with earlier predictions [34,35].

On the other hand, at large values of t, when the nuclear asymmetry is dominated by the incoherent contribution, $A_{\rm LU}^A(\phi)/A_{\rm LU}^p(\phi)$ is significantly smaller than unity: $A_{\rm LU}^A(\phi)/A_{\rm LU}^p(\phi) = 0.66$–$0.74$, depending on the target nucleus. This deviation of $A_{\rm LU}^A(\phi)/A_{\rm LU}^p(\phi)$ from unity is a result of the neutron contribution: The negative neutron contribution ($F_{1n} < 0$) decreases the numerator of $A_{\rm LU}^A$ and, at the same time, the positive neutron contribution $|\mathcal{T}_{\rm BH}^n|^2 + \mathcal{I}^n + |\mathcal{T}_{\rm DVCS}^n|^2$ increases the denominator of $A_{\rm LU}^A$. Since the effect of the deviation of $A_{\rm LU}^A(\phi)/A_{\rm LU}^p(\phi)$ from unity is so sizable, incoherent DVCS on nuclei gives a possibility to constrain neutron GPDs.

In this work, we considered one kind of DVCS observables, namely, the beam-spin asymmetry. We expect that for other DVCS asymmetries, such as, e.g., for the beam-charge DVCS asymmetry, the ratio of the nuclear to the free proton asymmetries will be qualitatively similar to $A_{\rm LU}^A(\phi)/A_{\rm LU}^p(\phi)$, see [35].

All results presented in this work, data grids for the dual parametrization of the nucleon GPDs and FORTRAN codes for various DVCS asymmetries measured in DVCS on nucleons and nuclei can be found and downloaded from the author's webpage `http://www.jlab.org/~vguzey`.

ACKNOWLEDGMENTS

We would like to thank H. Egiyan, F. X. Girod, H. Guler, K. Hafidi, D. Hash, M. Strikman, and H. Ye for useful and encouraging discussions. Authored by Jefferson Science Associates, LLC under U.S. DOE Contract No. DE-AC05-06OR23177.

APPENDIX: INPUT FOR CALCULATION OF DVCS ASYMMETRIES

In this appendix, we collect all expressions used in our numerical analysis of the nuclear and proton DVCS beam-spin asymmetries, see Eqs. (19), (20), and (21).

The interference, Bethe-Heitler and DVCS terms, which enter Eqs. (19), (20), and (21), read [10]

$$\begin{aligned}
\mathcal{I} &= \frac{\pm e^6}{xy^3 t\mathcal{P}_1(\phi)\mathcal{P}_2(\phi)}\big(c^{\mathcal{I}}_{0,\mathrm{unp}} + c^{\mathcal{I}}_{1,\mathrm{unp}}\cos(\phi) \\
&\quad + s^{\mathcal{I}}_{1,\mathrm{unp}}\sin(\phi)\big), \\
|\mathcal{T}_{\mathrm{BH}}|^2 &= \frac{e^6}{x^2y^2(1+\epsilon^2)^2 t\mathcal{P}_1(\phi)\mathcal{P}_2(\phi)}\big(c^{\mathrm{BH}}_{0,\mathrm{unp}} + c^{\mathrm{BH}}_{1,\mathrm{unp}}\cos(\phi) \\
&\quad + c^{\mathrm{BH}}_{2,\mathrm{unp}}\cos(2\phi)\big), \\
|\mathcal{T}_{\mathrm{DVCS}}|^2 &= \frac{e^6}{y^2Q^2}\, c^{\mathrm{DVCS}}_{0,\mathrm{unp}},
\end{aligned} \tag{A1}$$

where we have kept only twist-two terms and neglected the gluon GPDs. In Eq. (A1), $\mathcal{P}_1(\phi)$ and $\mathcal{P}_2(\phi)$ are lepton propagators; the plus sign in front of the interference term corresponds to electrons, while the minus sign is for positrons; ϕ is the angle between the lepton and production planes; the coefficients $c^I_{0,1,\mathrm{unp}}$, $s^I_{1,\mathrm{unp}}$, $c^{\mathrm{BH}}_{0,1,2}$, and $c^{\mathrm{DVCS}}_{0,\mathrm{unp}}$ are called harmonics.

When Eq. (A1) is applied to the coherent-enriched contribution, it should be evaluated with $x = x_A$ and the corresponding nuclear harmonics (see below). When Eq. (A1) is used to calculate the incoherent contribution, it should be evaluated with with $x = x_B$ and with the free proton and neutron harmonics (see below).

A. Nuclear part

Expressions for the $\cos\phi$ and $\sin\phi$ harmonics of a spin-0 zero nucleus are the same as for the pion case [53] after the replacement of the pion GPD and the electric form factor by their nuclear counterparts (one has also divide the pion harmonics involving GPDs by the factor of x due to a different normalization of the interference and DVCS terms used in [53]). The required harmonics read

$$\begin{aligned}
c^{\mathcal{I}}_{0,\mathrm{unp}} &= -8\frac{t}{Q^2}(2-y)\,[(2-x_A)(1-y) \\
&\quad -(1-x_A)(2-y)^2\left(1-\frac{t_{\min}}{t}\right)\Big] Z F_A(t)\Re e\mathcal{H}_A, \\
c^{\mathcal{I}}_{1,\mathrm{unp}} &= -8\,K(2-2y+y^2)Z F_A(t)\Re e\mathcal{H}_A, \\
s^{\mathcal{I}}_{1,\mathrm{unp}} &= 8K\,\lambda y(2-y)\,Z F_A(t)\Im m\mathcal{H}_A, \\
c^{\mathrm{BH}}_{0,\mathrm{unp}} &= \Big\{((2-y)^2 + y^2(1+\epsilon^2)^2) \\
&\quad \times\left[4x_A^2\frac{M_A^2}{t} + 4(1-x_A) + (4x_A+\epsilon^2)\frac{t}{Q^2}\right] \\
&\quad + 32\,x_A^2K^2\frac{M_A^2}{t} + 2\epsilon^2\left[4(1-y)(3+2\epsilon^2)\right. \\
&\quad \left. + y^2(2-\epsilon^4)\right] - 4x_A^2(2-y)^2(2+\epsilon^2)\frac{t}{Q^2}\Big\} Z^2F_A^2(t), \\
c^{\mathrm{BH}}_{1,\mathrm{unp}} &= -8\,K\,(2-y)\left(2\,x_A + \epsilon^2 - 4\,x_A^2\frac{M_A^2}{t}\right) Z^2F_A^2(t), \\
c^{\mathrm{BH}}_{2,\mathrm{unp}} &= 32\,K^2\,x_A^2\frac{M_A^2}{t}\,Z^2F_A^2(t), \\
c^{\mathrm{DVCS}}_{0,\mathrm{unp}} &= 2(2-2y+y^2)|\mathcal{H}_A|^2,
\end{aligned} \tag{A2}$$

where K is the so-called kinematic K-factor [10]; λ is the incoming lepton helicity.

The nuclear form factor F_A entering Eq. (A2) is evaluated at $t' = A/(A-1)t$ for the coherent-enriched contribution and at t for the purely coherent case.

For ^{4}He, the nuclear form factor is parameterized as

$$F_A(t) = (1-(a^2t)^6)e^{-b^2|t|}, \tag{A3}$$

where $a = 0.316$ fm and $b = 0.681$ fm [49].

For other nuclei used in this paper, the nuclear form factor is defined as

$$F_A(t) = 4\pi\int_0^\infty dr\, r\frac{\sin(\sqrt{|t|}r)}{\sqrt{|t|}}\rho_A(r), \tag{A4}$$

where $\rho_A(r)$ is the nuclear charge density distribution taken in the following form [50]:

Nitrogen ($A = 14$, $Z = 7$):

$$\begin{aligned}
w &= -0.18, \quad z = 0.505, \\
c &= 2.57, \quad \rho_0 = 0.0127908, \\
\rho_A(r) &= \rho_0\frac{1+w\frac{r^2}{c^2}}{1+e^{(r-c)/z}}.
\end{aligned} \tag{A5}$$

Neon ($A = 20$, $Z = 10$):

$$\begin{aligned}
z &= 0.571, \quad c = 2.805, \\
\rho_0 &= 0.00767524, \\
\rho_A(r) &= \rho_0\frac{1}{1+e^{(r-c)/z}}.
\end{aligned} \tag{A6}$$

Krypton ($A = 84$, $Z = 36$):

$$\begin{aligned}
z &= 0.496, \quad c = 4.83, \\
\rho_0 &= 0.00191897, \\
\rho_A(r) &= \rho_0\frac{1}{1+e^{(r-c)/z}}.
\end{aligned} \tag{A7}$$

Xenon ($A = 131$, $Z = 54$):

$$\begin{aligned}
w &= 0.3749, \quad z = 2.6776, \\
c &= 5.3376, \quad \rho_0 = 0.00112617, \\
\rho_A(r) &= \rho_0\frac{1+w\frac{r^2}{c^2}}{1+e^{(r^2-c^2)/z^2}}.
\end{aligned} \tag{A8}$$

B. Proton part

Expressions for the required $\cos\phi$ and $\sin\phi$ harmonics for the proton target are derived in [10]

$$\begin{aligned}
c^{\mathcal{I}}_{0,\mathrm{unp}} &= -8\,(2-y)\Re e\left[\frac{(2-y)^2}{1-y}K^2C^{\mathcal{I}}_{\mathrm{unp}}\right. \\
&\quad \left. + \frac{t}{Q^2}(1-y)(2-x_B)\big(C^{\mathcal{I}}_{\mathrm{unp}} + \Delta C^{\mathcal{I}}_{\mathrm{unp}}\big)\right], \\
c^{\mathcal{I}}_{1,\mathrm{unp}} &= -8\,K(2-2y+y^2)\Re e C^{\mathcal{I}}_{\mathrm{unp}},
\end{aligned}$$

$$
\begin{aligned}
s^{\mathcal{I}}_{1,\mathrm{unp}} &= 8K\,\lambda y(2-y)\Im m\, C^{\mathcal{I}}_{\mathrm{unp}},\\
c^{\mathrm{BH}}_{0,\mathrm{unp}} &= 8\,K^2\left[(2+3\epsilon^2)\frac{Q^2}{t}\left(F_{1p}^2-\frac{t}{4m_N^2}F_{2p}^2\right)\right.\\
&\quad\left.+2x_B^2\left(F_{1p}+F_{2p}\right)^2\right]+(2-y)^2\\
&\quad\times\left\{(2+\epsilon^2)\left[\frac{4x_B^2m_N^2}{t}\left(1+\frac{t}{Q^2}\right)^2\right.\right.\\
&\quad\left.+4(1-x_B)\left(1+x_B\frac{t}{Q^2}\right)\right]\left(F_{1p}^2-\frac{t}{4m_N^2}F_{2p}^2\right)\\
&\quad+4x^2\left[x_B+\left(1-x_B+\frac{\epsilon^2}{2}\right)\left(1-\frac{t}{Q^2}\right)^2\right.\\
&\quad\left.\left.-x_B(1-2x_B)\frac{t^2}{Q^4}\right]\left(F_{1p}+F_{2p}\right)^2\right\}\\
&\quad+8(1+\epsilon^2)\left(1-y-\frac{\epsilon^2y^2}{4}\right)\\
&\quad\times\left[2\epsilon^2\left(1-\frac{t}{4m_N^2}\right)\left(F_{1p}^2-\frac{t}{4m_N^2}F_{2p}^2\right)\right.\\
&\quad\left.-x_B^2\left(1-\frac{t}{Q^2}\right)^2\left(F_{1p}+F_{2p}\right)^2\right],\\
c^{\mathrm{BH}}_{1,\mathrm{unp}} &= 8\,K\,(2-y)\left\{\left(\frac{4x_B^2m_N^2}{t}-2x_B-\epsilon^2\right)\right.\\
&\quad\times\left(F_{1p}^2-\frac{t}{4m_N^2}F_{2p}^2\right)+2x_B^2\left(1-(1-2x_B)\frac{t}{Q^2}\right)\\
&\quad\left.\times\left(F_{1p}+F_{2p}\right)^2\right\},\\
c^{\mathrm{BH}}_{2,\mathrm{unp}} &= 8\,x_B^2\,K^2\left\{\frac{4m_N^2}{t}\left(F_{1p}^2-\frac{t}{4m_N^2}F_{2p}^2\right)\right.\\
&\quad\left.+2\left(F_{1p}+F_{2p}\right)^2\right\},\\
c^{\mathrm{DVCS}}_{0,\mathrm{unp}} &= 2(2-2y+y^2)C^{\mathrm{DVCS}}_{\mathrm{unp}},
\end{aligned}
\tag{A9}
$$

where

$$
\begin{aligned}
C^{\mathcal{I}}_{\mathrm{unp}} &= F_{1p}\,\mathcal{H}_p-\frac{t}{4m_N^2}F_{2p}\mathcal{E}_p,\\
\Delta C^{\mathcal{I}}_{\mathrm{unp}} &= -\frac{x_B^2}{(2-x_B)^2}(F_{1p}+F_{2p})(\mathcal{H}_p+\mathcal{E}_p),\\
C^{\mathrm{DVCS}}_{\mathrm{unp}} &= \frac{1}{(2-x_B)^2}\left[4(1-x_B)|\mathcal{H}_p|^2-x_B^2(\mathcal{H}_p^*\mathcal{E}_p+\mathcal{E}_p^*\mathcal{H}_p)\right.\\
&\quad\left.-\left(x_B^2+(2-x_B)^2\frac{t}{4m_N^2}\right)|\mathcal{E}_p|^2\right].
\end{aligned}
\tag{A10}
$$

Equations (A9) and (A10) involve proton Compton form factors (CFFs) $\mathcal{H}_p$ and $\mathcal{E}_p$ and electromagnetic form factors F_{1p} and F_{2p}. For the CFFs, we used the dual parametrization with $J_u = J_d = 0$ [46]. The proton electromagnetic form factors are parameterized in the following form [10]:

$$
\begin{aligned}
F_{1p}(t) &= \frac{1-(1+k_p)\frac{t}{4m_N^2}}{1-\frac{t}{4m_N^2}}G_D(t),\\
F_{2p}(t) &= \frac{k_p}{1-\frac{t}{4m_N^2}}G_D(t),\\
G_D(t) &= \frac{1}{1-\frac{t}{m_V^2}},
\end{aligned}
\tag{A11}
$$

where k_p is the proton anomalous magnetic moment, $k_p = 1.79$; $m_V = 0.84$ GeV. More elaborate parametrizations of the nucleon elastic form factors are possible, see, e.g., [54], but Eq. (A11) is sufficiently accurate for our purposes.

C. Neutron part

Expressions for the $\cos\phi$ and $\sin\phi$ harmonics for the neutron case are readily obtained from Eqs. (A9) and (A10) by replacing the proton CFFs and electromagnetic form factors by their neutron counterparts. The neutron CFFs are obtained from the proton ones by exchanging $e_u \leftrightarrow e_d$ in the DVCS amplitude.

The neutron electromagnetic form factors are parameterized in the following form [10]:

$$
\begin{aligned}
F_{1n}(t) &= -\frac{t}{4m_N^2}\frac{k_n}{1-\frac{t}{4m_N^2}}G_D(t),\\
F_{2n}(t) &= \frac{k_n}{1-\frac{t}{4m_N^2}}G_D(t),
\end{aligned}
\tag{A12}
$$

where k_n is the neutron anomalous magnetic moment, $k_n = -1.91$.

[1] D. Mueller, D. Robaschik, B. Geyer, F. M. Dittes, and J. Horejsi, Fortschr. Phys. **42**, 101 (1994).
[2] X. D. Ji, Phys. Rev. D **55**, 7114 (1997).
[3] X. D. Ji, J. Phys. G **24**, 1181 (1998).
[4] A. V. Radyushkin, Phys. Lett. **B380**, 417 (1996).
[5] A. V. Radyushkin, Phys. Rev. D **56**, 5524 (1997).
[6] A. V. Radyushkin, arXiv:hep-ph/0101225.
[7] S. J. Brodsky, L. Frankfurt, J. F. Gunion, A. H. Mueller, and M. Strikman, Phys. Rev. D **50**, 3134 (1994).
[8] K. Goeke, M. V. Polyakov, and M. Vanderhaeghen, Prog. Part. Nucl. Phys. **47**, 401 (2001).
[9] M. Diehl, T. Feldmann, R. Jakob, and P. Kroll, Nucl. Phys. **B596**, 33 (2001); [Erratum-*ibid.* **B605**, 647 (2001)].
[10] A. V. Belitsky, D. Mueller, and A. Kirchner, Nucl. Phys. **B629**, 323 (2002).
[11] M. Diehl, Phys. Rep. **388**, 41 (2003).
[12] A. V. Belitsky and A. V. Radyushkin, Phys. Rep. **418**, 1 (2005).

[13] J. C. Collins and A. Freund, Phys. Rev. D **59**, 074009 (1999).
[14] J. C. Collins, L. Frankfurt, and M. Strikman, Phys. Rev. D **56**, 2982 (1997).
[15] L. Mankiewicz, G. Piller, and A. Radyushkin, Eur. Phys. J. C **10**, 307 (1999).
[16] L. L. Frankfurt, P. V. Pobylitsa, M. V. Polyakov, and M. Strikman, Phys. Rev. D **60**, 014010 (1999).
[17] M. V. Polyakov and S. Stratmann, arXiv:hep-ph/0609045.
[18] M. V. Polyakov, Nucl. Phys. **B555**, 231 (1999).
[19] M. Diehl, T. Gousset, B. Pire, and O. V. Terayev, arXiv:hep-ph/9901233.
[20] E. R. Berger, M. Diehl, and B. Pire, Eur. Phys. J. C **23**, 675 (2002).
[21] E. R. Berger, M. Diehl, and B. Pire, Phys. Lett. **B523**, 265 (2001).
[22] M. Diehl, T. Gousset, and B. Pire, Phys. Rev. D **62**, 073014 (2000).
[23] M. V. Polyakov, Phys. Lett. **B555**, 57 (2003).
[24] V. Guzey and M. Siddikov, J. Phys. G **32**, 251 (2006).
[25] A. Freund and M. Strikman, Phys. Rev. C **69**, 015203 (2004).
[26] A. Freund and M. Strikman, Eur. Phys. J. C **33**, 53 (2004).
[27] F. Cano and B. Pire, Eur. Phys. J. A **19**, 423 (2004).
[28] P. V. Pobylitsa, Phys. Rev. D **67**, 094012 (2003).
[29] B. C. Tiburzi and G. A. Miller, Phys. Rev. D **67**, 113004 (2003).
[30] B. C. Tiburzi, W. Detmold, and G. A. Miller, Phys. Rev. D **70**, 093008 (2004).
[31] S. Scopetta and V. Vento, Phys. Rev. D **69**, 094004 (2004).
[32] S. Noguera, S. Scopetta, and V. Vento, Phys. Rev. D **70**, 094018 (2004).
[33] E. R. Berger, F. Cano, M. Diehl, and B. Pire, Phys. Rev. Lett. **87**, 142302 (2001).
[34] A. Kirchner and D. Mueller, Eur. Phys. J. C **32**, 347 (2003).
[35] V. Guzey and M. Strikman, Phys. Rev. C **68**, 015204 (2003).
[36] F. Cano and B. Pire, Nucl. Phys. **A711**, 133 (2002).
[37] F. Cano and B. Pire, Nucl. Phys. **A721**, 789 (2003).
[38] S. Scopetta, Phys. Rev. C **70**, 015205 (2004).
[39] S. Scopetta, Nucl. Phys. **A790**, 364 (2007).
[40] S. Liuti and S. K. Taneja, Phys. Rev. C **72**, 032201(R) (2005).
[41] S. Liuti and S. K. Taneja, Phys. Rev. C **72**, 034902 (2005).
[42] F. Ellinghaus, R. Shanidze, and J. Volmer (HERMES Collaboration), AIP Conf. Proc. **675**, 303 (2003), arXiv:hep-ex/0212019.
[43] F. Ellinghaus, arXiv:0710.5768 [hep-ex].
[44] M. Mazouz *et al*. (Jefferson Lab Hall A Collaboration), Phys. Rev. Lett. **99**, 242501 (2007).
[45] L. Frankfurt, V. Guzey, M. Strikman, and M. Zhalov, JHEP 08 (2003) 043.
[46] V. Guzey and T. Teckentrup, Phys. Rev. D **74**, 054027 (2006).
[47] M. V. Polyakov and A. G. Shuvaev, arXiv:hep-ph/0207153.
[48] M. V. Polyakov and M. Vanderhaeghen, arXiv:0803.1271 [hep-ph].
[49] R. F. Frosch, J. S. McCarthy, R. E. Rand, and M. R. Yearian, Phys. Rev. **160**, 874 (1967).
[50] C. W. De Jager, H. De Vries, and C. De Vries, At. Data Nucl. Data Tables **36**, 495 (1987).
[51] L. Frankfurt, G. A. Miller, and M. Strikman, Phys. Rev. D **65**, 094015 (2002).
[52] K. Hafidi *et al*., Jefferson Lab Experiment E08-024 (2008).
[53] A. V. Belitsky, D. Muller, A. Kirchner, and A. Schafer, Phys. Rev. D **64**, 116002 (2001).
[54] R. Bradford, A. Bodek, H. Budd, and J. Arrington, Nucl. Phys. Proc. Suppl. **159**, 127 (2006).